Reconstruction algorithm and phase calibration of phase contrast imaging

小组成员：王　菲 陈佳琦 谢铭效

1 Phase Reconstruction

Phase/Complex Difference Reconstruction

Defination of the aliasing velocity (VENC)

$$\mathrm{VENC} = \frac{\pi}{\gamma|\Delta m_1|}$$

where Δm_1 is the change in the first moment of the bipolar velocity gradient

Assume that

$$Z_1 = x_1 + iy_1 = \rho_1 e^{i\phi_1}$$

$$Z_2 = x_2 + iy_2 = \rho_2 e^{i\phi_2}$$

Phase Difference Reconstruction

$$\Delta\phi = \angle\left(\sum_j \frac{Z_{1j} Z_{2j}^*}{\sigma_j^2}\right)$$

For mutiple coils (Phase arrays)

$$\Delta\phi = \gamma \Delta m_1 v = \frac{v}{\mathrm{VENC}}\pi$$

Complex Difference Reconstruction

$$CD = \sqrt{|Z_1|^2 + |Z_2|^2 - 2|Z_1||Z_2|\cos(\Delta\phi)}$$

$$CD_{corr} = \sqrt{|Z_1|^2 + |Z_2|^2 - 2|Z_1||Z_2|\cos(\Delta\phi_{corr})}$$

$$CD = 2M\left|\sin\left(\frac{\pi v}{2\,\mathrm{VENC}}\right)\right|$$

Bernstein, M. A., King, K. F., & Zhou, X. J. (2004). Handbook of MRI pulse sequences. *Elsevier Academic Press*.

Phase/Complex Difference Reconstruction

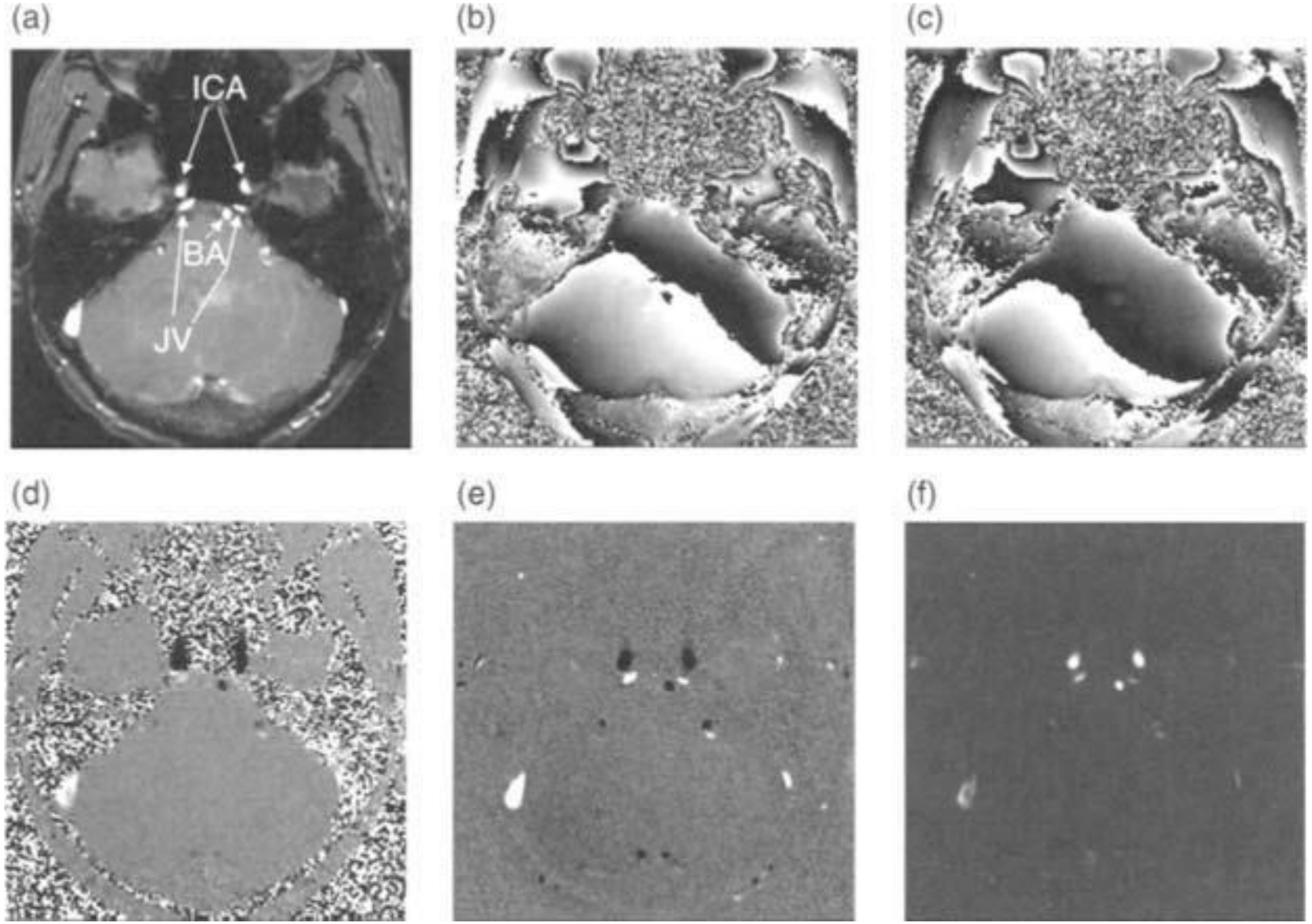

Phase Difference Reconstruction

Complex Difference Reconstruction

Bernstein, M. A., King, K. F., & Zhou, X. J. (2004). Handbook of MRI pulse sequences. *Elsevier Academic Press*.

Eddy Current

- Faraday's law
- proportional to the gradient slew rate

The cancellation concept

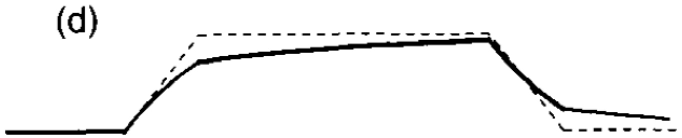

plateau length and the decay rate of eddy current

Waveform Preemphasis

intentionally distort the current waveform

Eddy-Current Spatial Dependence

$$B_e(\vec{x}, t) = b_0(t) + \vec{x} \cdot \vec{g}(t) + \cdots$$

a spherical harmonic expansion

Shielded Gradient Coils

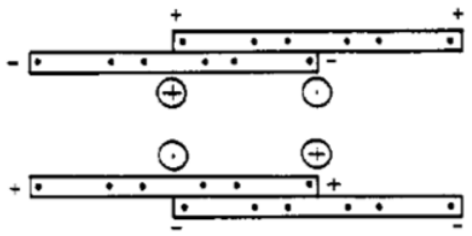

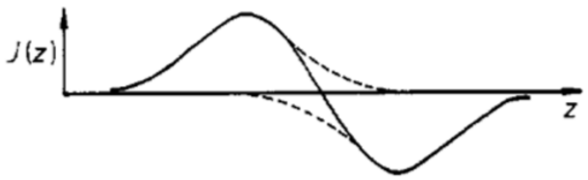

Eddy-Current Time Dependence

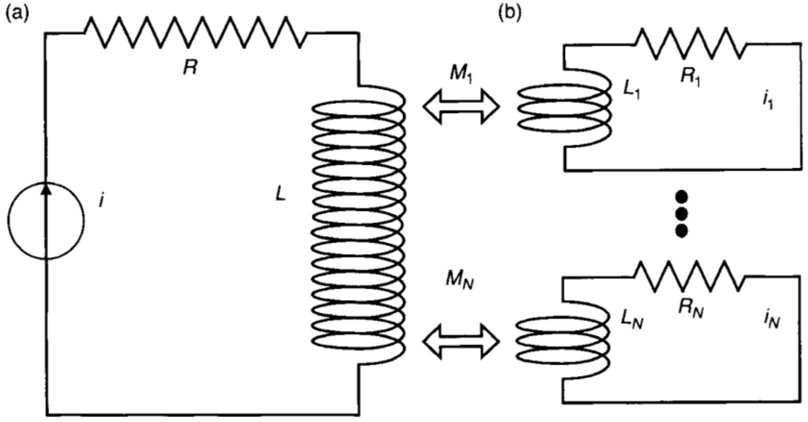

moving /using multiple samples

Preemphasis Compensation

Linear component

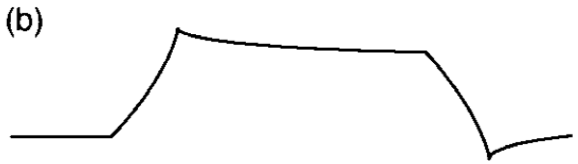

Preemphasized(high-pass-filtered) waveform.

B_0 component

$$g(t) = -\frac{dG}{dt} \otimes e(t)$$

$$e(t) = H(t) \sum_n \alpha_n e^{-t/\tau_n}$$

using a B_0 coil with current control that can be varied in real time or shifting the exciter / receiver frequency

Gradient Waveform De-rating

Decreasing the amplitude of the trapezoid while holding the slew rate fixed

Bernstein, M. A., King, K. F., & Zhou, X. J. (2004). Handbook of MRI pulse sequences. *Elsevier Academic Press*.
Mansfield, P., & Chapman, B. (1986). Active magnetic screening of coils for static and time-dependent magnetic field generation in NMR imaging. *Journal of Physics E: Scientific Instruments, 19*(7), 540-545. doi:10.1088/0022-3735/19/7/008

B_0 concomitant field

spatiotemporally varying 3D fields

$$\boldsymbol{B}(x,y,z,t) = [B_x(x,y,z,t), B_y(x,y,z,t), B_z(x,y,z,t)]$$

The overall magnetic field

$$B_{c,0th}(t) = \frac{z_0^2\left(G_x^2(t) + G_y^2(t)\right)}{2B_0}$$

the new demodulation frequency

$$\begin{aligned} f_{new}(t) &= f_0 + \Delta f_{c,0th}(t) \\ &= \frac{\gamma}{2\pi}B_0 + \frac{\gamma}{2\pi}\left(G_x^2(t) + G_y^2(t)\right)z_0^2/2B_0 \end{aligned}$$

- created simultaneously with the spatial encoding gradient fields
- accumulate undesired phase within k-space data
- results in image blurring and spatial shifts

Weavers, P. T., Tao, S., Trzasko, J. D., Frigo, L. M., Shu, Y., Frick, M. A., . . . Bernstein, M. A. (2018). B0 concomitant field compensation for MRI systems employing asymmetric transverse gradient coils. *Magnetic Resonance in Medicine, 79*(3), 1538-1544. doi:10.1002/mrm.26790

B_0 concomitant field

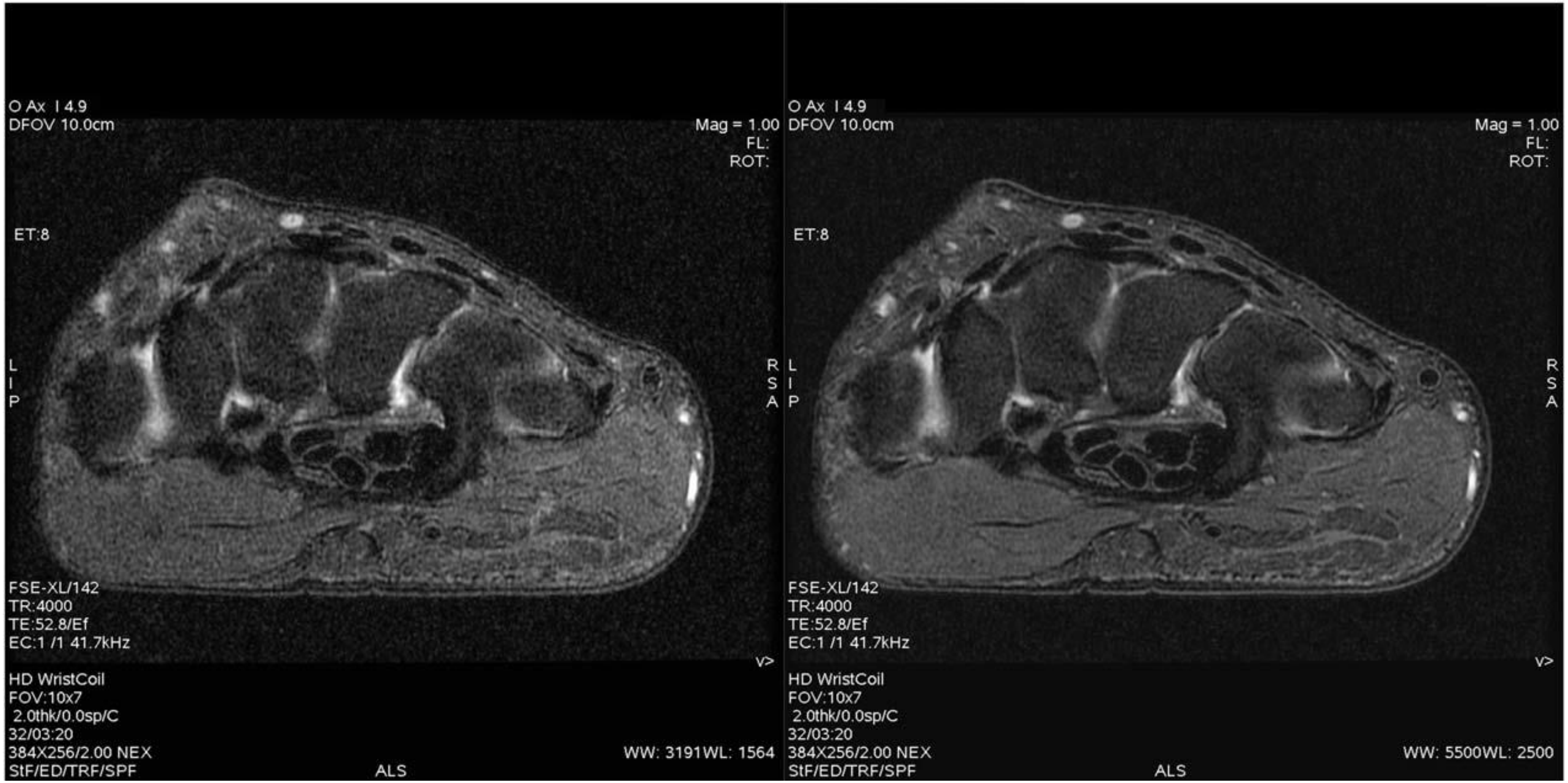

Weavers, P. T., Tao, S., Trzasko, J. D., Frigo, L. M., Shu, Y., Frick, M. A., . . . Bernstein, M. A. (2018). B0 concomitant field compensation for MRI systems employing asymmetric transverse gradient coils. *Magnetic Resonance in Medicine, 79*(3), 1538-1544. doi:10.1002/mrm.26790

Phase cycling

$$\underbrace{\frac{1}{2}\left\|y - A\left(Mm \cdot e^{\imath Pp}\right)\right\|_2^2}_{\text{Data consistency } f(m,p)} + \underbrace{g_m(m) + g_p(p)}_{\text{Regularization } g(m,p)}$$

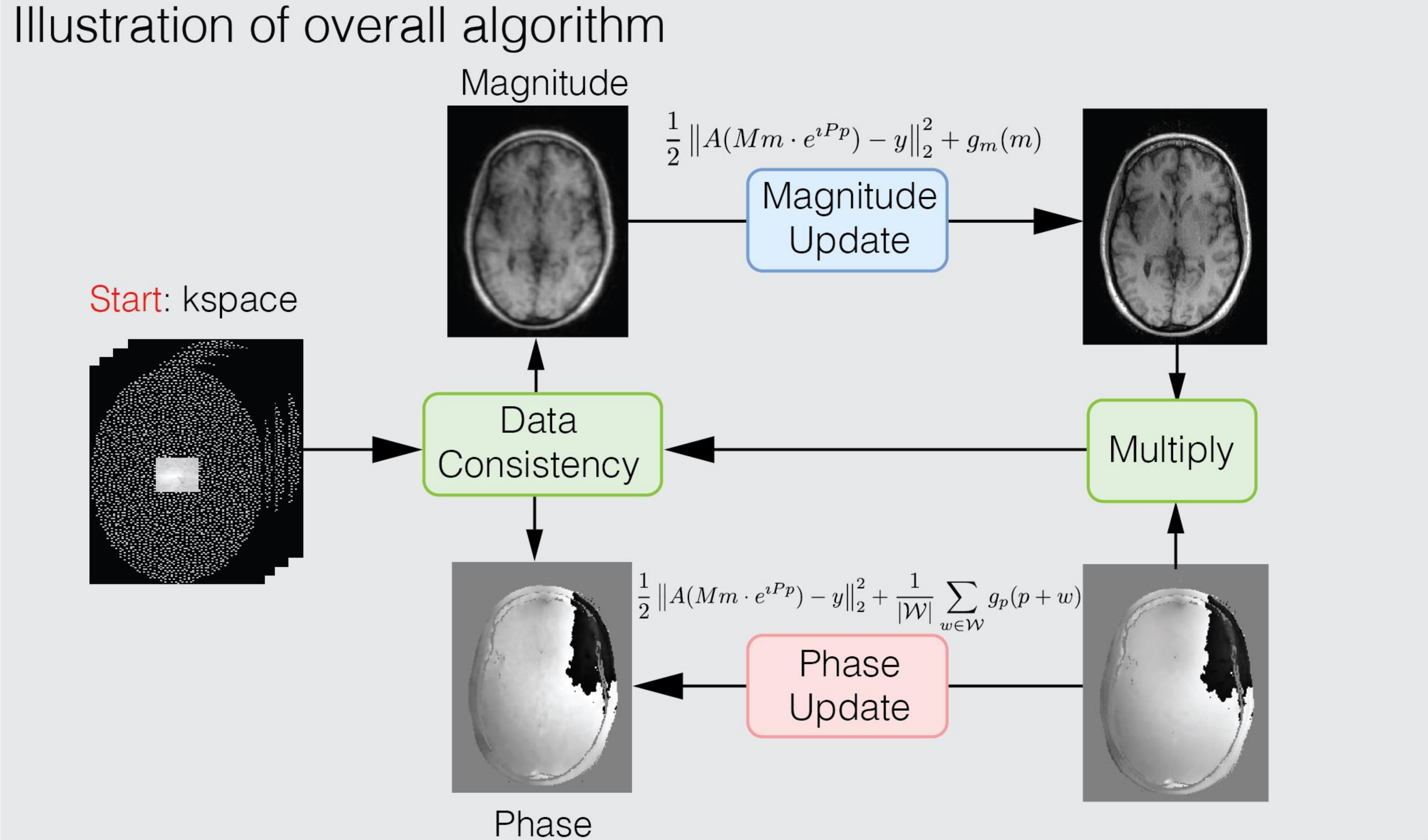

Ong, F., Cheng, J., & Lustig, M. (2017). General Phase Regularized Reconstruction using Phase Cycling. *arXiv e-prints*. Retrieved from https://ui.adsabs.harvard.edu/abs/2017arXiv170905374O

Phase cycling

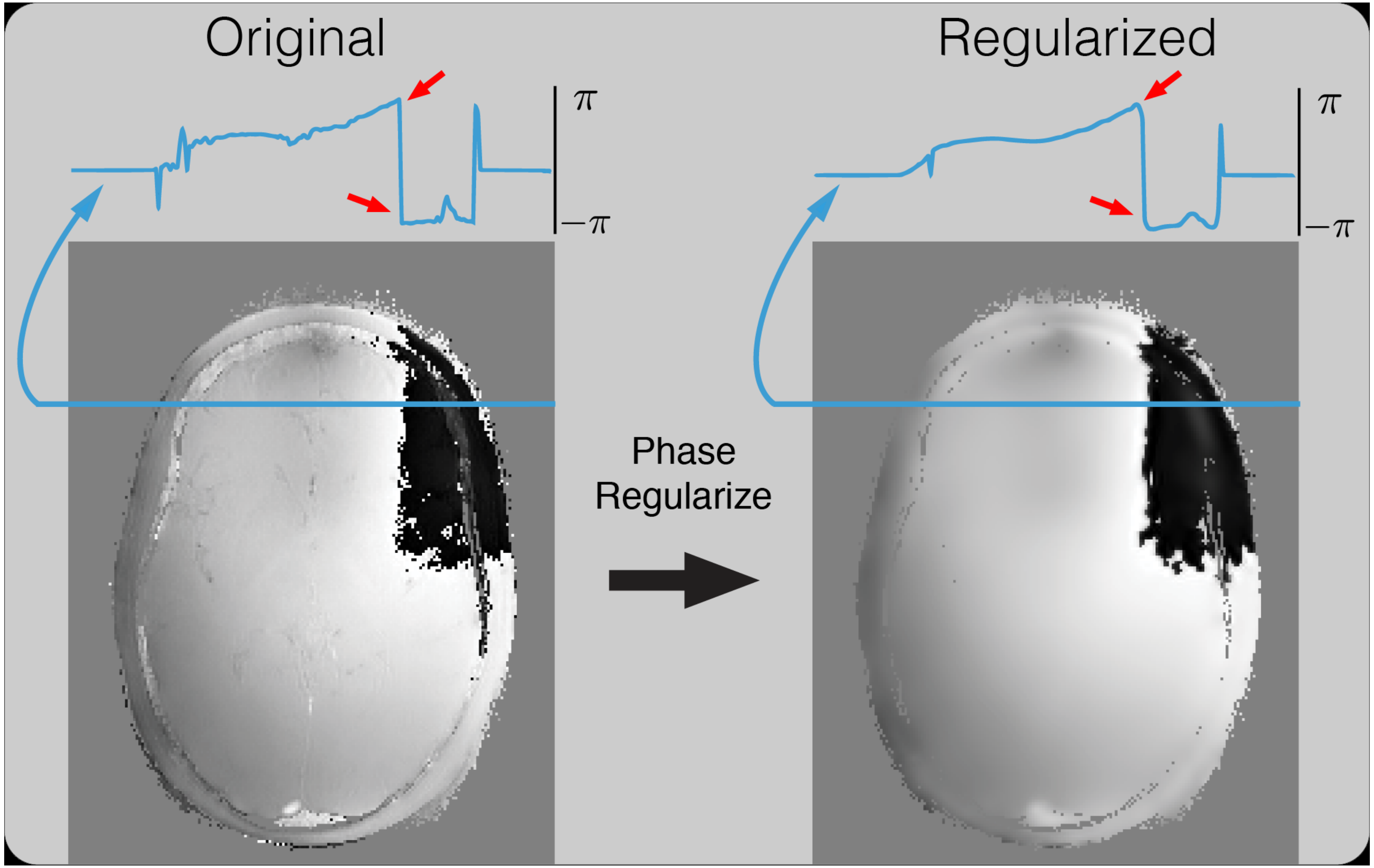

Ong, F., Cheng, J., & Lustig, M. (2017). General Phase Regularized Reconstruction using Phase Cycling. *arXiv e-prints*. Retrieved from https://ui.adsabs.harvard.edu/abs/2017arXiv170905374O

Phase cycling

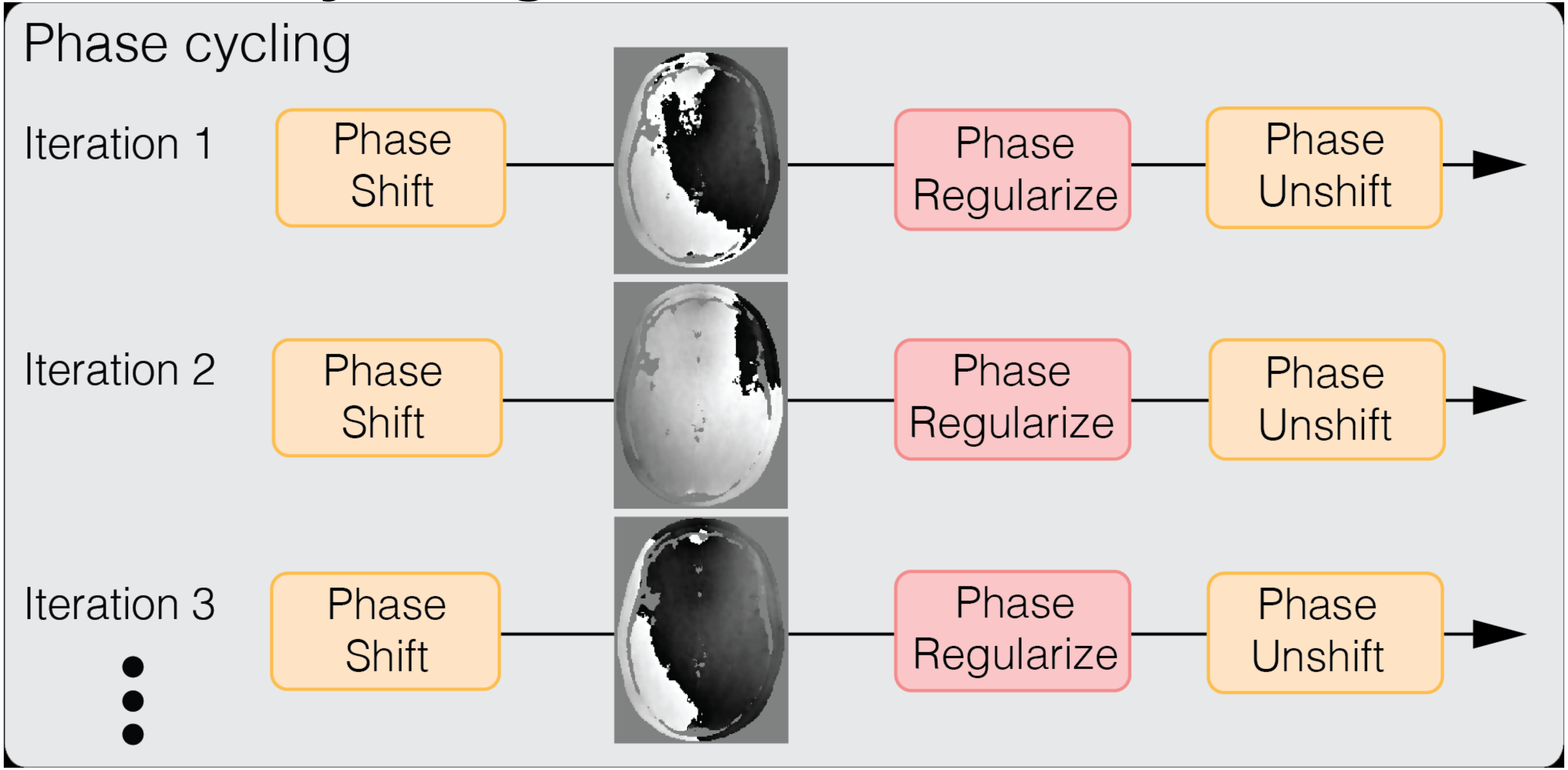

Ong, F., Cheng, J., & Lustig, M. (2017). General Phase Regularized Reconstruction using Phase Cycling. *arXiv e-prints*. Retrieved from https://ui.adsabs.harvard.edu/abs/2017arXiv170905374O

Partial Fourier

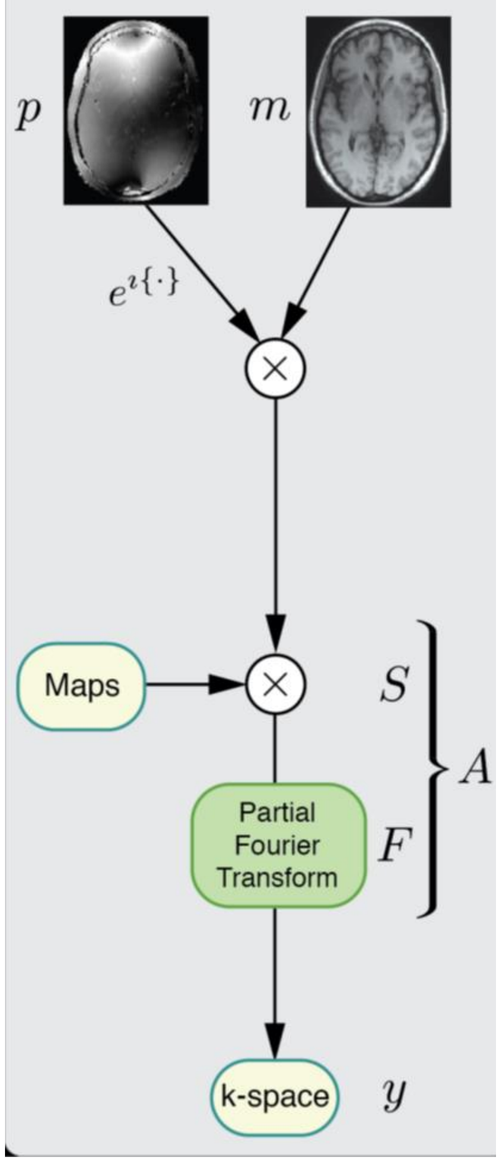

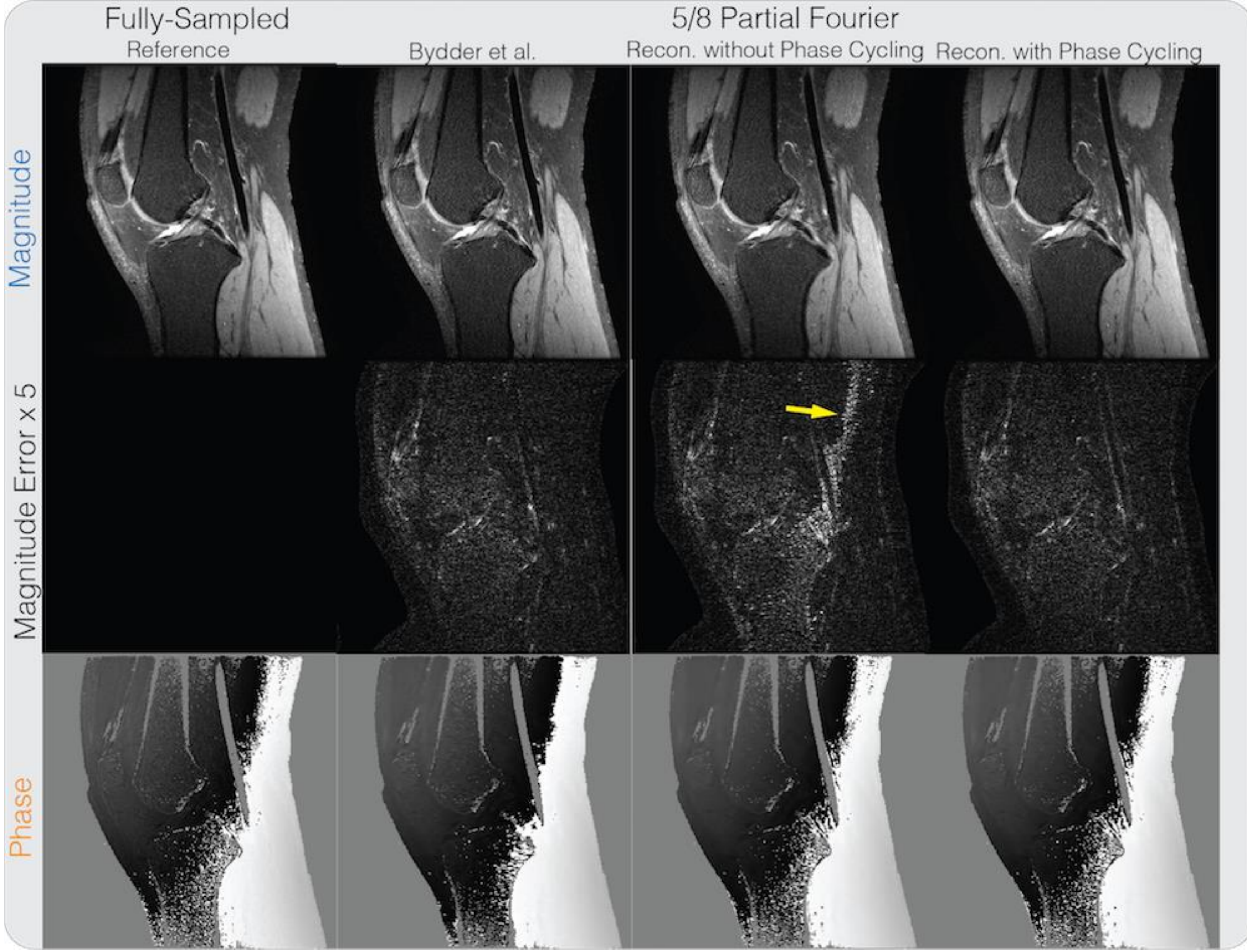

Ong, F., Cheng, J., & Lustig, M. (2017). General Phase Regularized Reconstruction using Phase Cycling. *arXiv e-prints*. Retrieved from https://ui.adsabs.harvard.edu/abs/2017arXiv170905374O

2 Phase Calibration

Partial Volume Effects

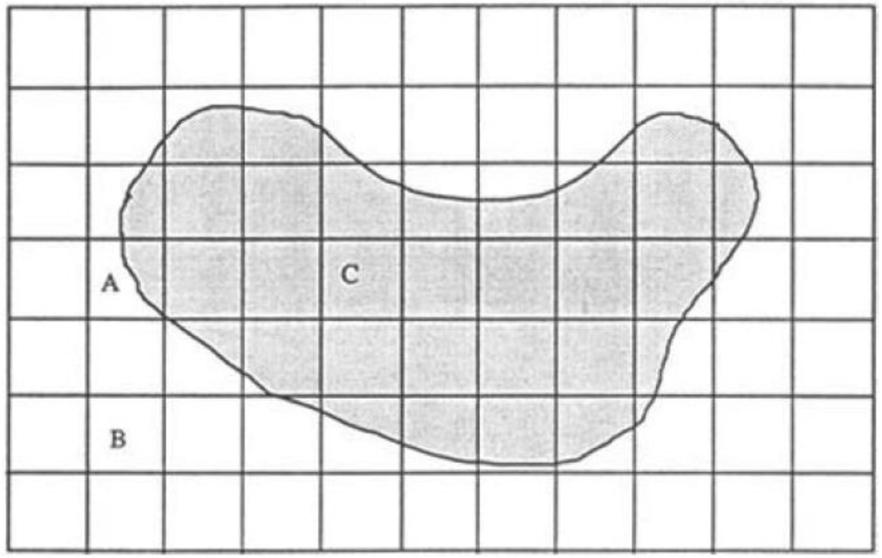

Figure 2. Schematic illustrates the partial-volume effect. Two different tissues are represented by the shaded and the unshaded areas. Voxels such as *B* and *C* include only one tissue. Voxels such as *A*, which are called partially occupied voxels, include more than one type of tissue.

- The relative signal intensity and volume fraction of flowing and stationary spins
- The flow type (plug or laminar flow)
- The relative size of the vessel and voxel grid
- The angulation between flow direction, velocity encoding direction and voxel grid
- The relative positions of the vessel cross section and voxel grids

Tang, C. , Blatter, D. D. and Parker, D. L. (1993), Accuracy of phase-contrast flow measurements in the presence of partial-volume effects. J. Magn. Reson. Imaging, 3: 377-385.

Partial Volume Effects

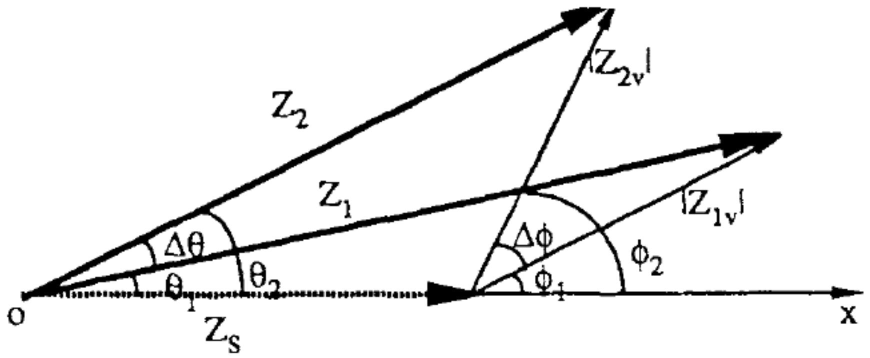

Figure 3. Magnetization vector obtained from two flow measurements. Z_1 and Z_2 are the total magnetization vectors for two flow measurements, respectively. Z_S (dotted line) is the magnetization of stationary spins. Z_{1v} and Z_{2v} are the magnetization vectors for flowing spins in the two acquisitions, respectively. $\Delta\theta$ is the measured phase shift. $\Delta\phi$ is the phase shift of flowing spins.

$$Z_{1v} = \int \rho_{(v_z)} \exp\left(ik_1 v_z\right) dv_z$$

$$Z_{2v} = \int \rho_{(v_z)} \exp\left(ik_2 v_z\right) dv_z$$

$$\theta_1 = \arctan\left[\frac{|Z_{1v}| sin\varphi_1}{|Z_{1v}| cos\varphi_1 + |Z_s|}\right]$$

$$\theta_2 = \arctan\left[\frac{|Z_{2v}| sin\varphi_2}{|Z_{2v}| cos\varphi_2 + |Z_s|}\right]$$

$$\Delta\theta = \theta_1 - \theta_2$$

$$v_i = \frac{\Delta\theta}{\pi} VENC$$

$$Q_i = \Delta s v_i$$

$$Q_m = \sum_i Q_i$$

Tang, C. , Blatter, D. D. and Parker, D. L. (1993), Accuracy of phase-contrast flow measurements in the presence of partial-volume effects. J. Magn. Reson. Imaging, 3: 377-385.

Partial Volume Effects: Calibration -Correction Factor

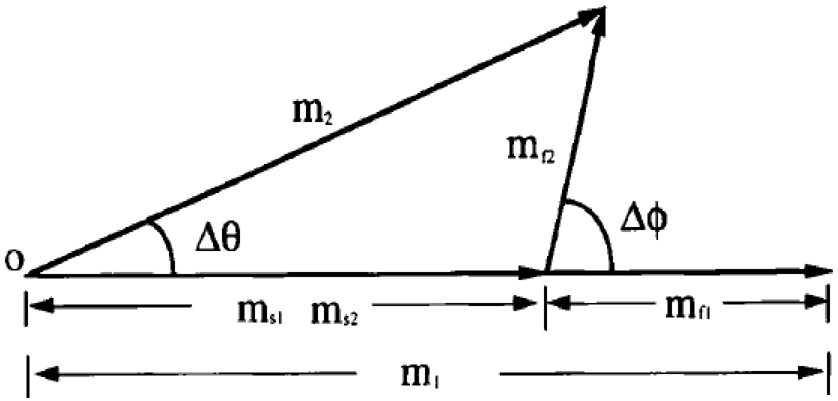

Figure 1. Illustration of the change in transverse magnetization between the two velocity-encoding acquisitions. m_{s1} and m_{s2} are the transverse magnetizations of stationary spins, and m_{f1} and m_{f2} are the transverse magnetizations of flowing spins; m_1 and m_2 are the total transverse magnetizations in the two acquisitions. Δϕ is the phase-shift difference of flowing spins between the two acquisitions, while Δθ is the phase shift actually measured between acquisitions.

$$\Delta s_f = \eta \Delta s$$

$$\Delta s_s = (1-\eta)\Delta s$$

$$Q_0 = v_{z0}\Delta s_f$$

$$m_f = \rho_f \Delta V_f$$

$$M_f = \rho_f \Delta V$$

$$Q = \frac{VENC\Delta s}{\pi}\arctan\left(\frac{m_f sin\Delta\varphi}{m_f cos\Delta\varphi + m_s}\right)$$

Small-phase-shift approximation:

$$Q = v_{z0}\Delta s\frac{m_f}{m_f + m_s}$$

$$Q = Q_0\frac{M_f}{m}$$

$$Q_c = Q\frac{m}{M_f}$$

$$Q_{total} = \sum_{fully} Q_f + \sum_{partially}\frac{m_i}{M_f}Q_i$$

Tang, C. , Blatter, D. D. and Parker, D. L. (1995), Correction of partial-volume effects in phase-contrast flow measurements. J. Magn. Reson. Imaging, 5: 175-180.

Partial Volume Effects: Calibration

-Correction Factor

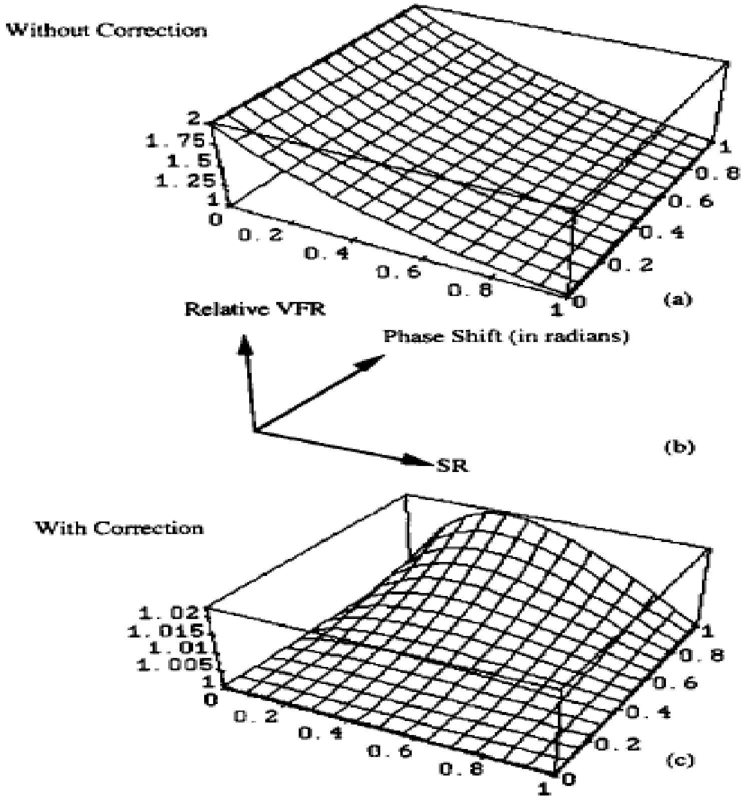

Figure 2. Relative VFR of a partially occupied voxel without *(a)* and with *(c)* correction. Half the voxel is occupied by stationary spins and half by flowing spins. The relative VFR is plotted as function of SR and phase shift *(b)*. The VFR is overestimated by as much as 100%. After correction, the error is less than 2%.

$$\frac{Q}{Q_0} = \frac{1}{\eta\Delta\varphi}\arctan\left[\frac{sin\Delta\varphi}{\frac{SR(1-\eta)}{\eta} + sin\Delta\varphi}\right]$$

$$\mathrm{SR} = \frac{\rho_s}{\rho_f}$$

$$\frac{Q_c}{Q_0} = \frac{\eta + (1-\eta)SR}{\eta\Delta\varphi}\arctan\left[\frac{sin\Delta\varphi}{\frac{SR(1-\eta)}{\eta} + sin\Delta\varphi}\right]$$

Tang, C. , Blatter, D. D. and Parker, D. L. (1995), Correction of partial-volume effects in phase-contrast flow measurements. J. Magn. Reson. Imaging, 5: 175-180.

Partial Volume Effects: Calibration

-Origin Translation

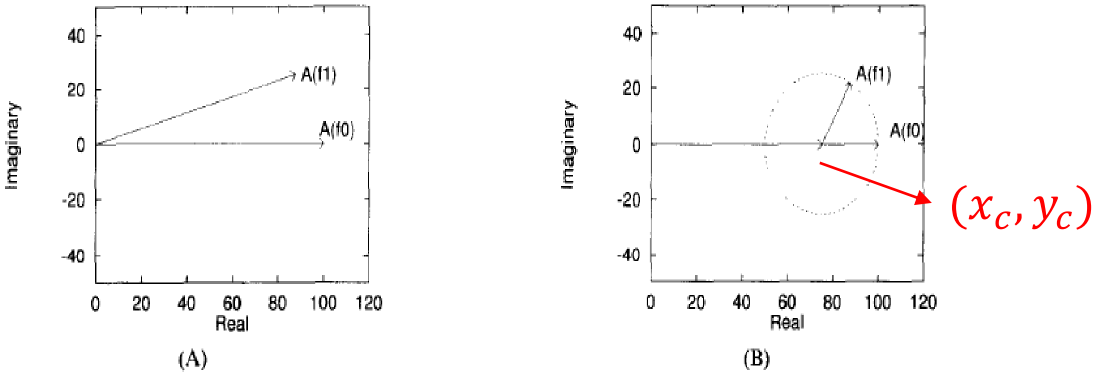

$$\mathrm{A(f)} = \mathrm{M}e^{j\Gamma}\int_{-V_m}^{V_m} p(v)e^{j2\pi f v}dv$$

$$f = \gamma G_v \tau T$$

$$\mathrm{A}(f_1) = 100[\frac{3}{4} + \frac{1}{4}e^{j(\pi/3)}]$$

$$\mathrm{A}(f_0) = 100$$

$$\mathrm{A}(f_0) = (x_0, y_0)$$

$$\mathrm{A}(f_1) = (x_1, y_1)$$

$$x_c = \frac{1}{2}\frac{(y_0 + y_1)(y_0 - y_1) + (x_0 + x_1)(x_0 - x_1)}{\left(\frac{y_1}{x_1}\right)(y_0 - y_1) + (x_0 - x_1)}$$

$$y_c = \frac{y_1}{x_1}x_c$$

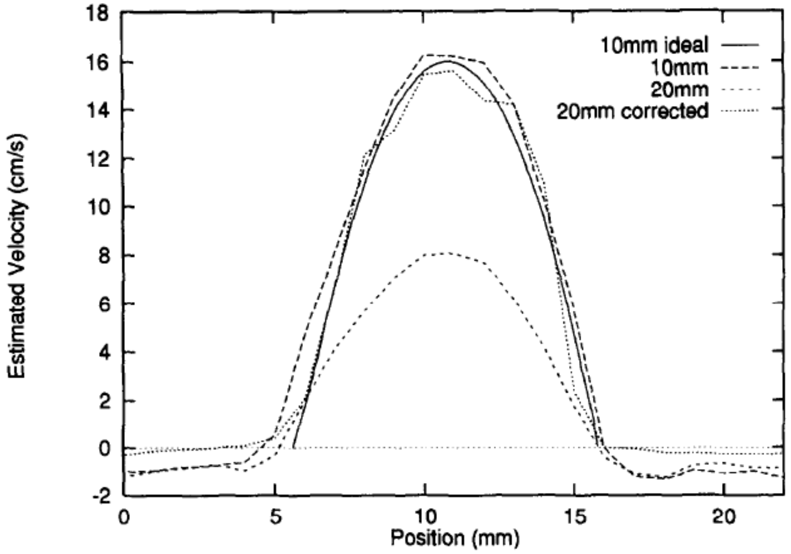

Hamilton, C. A. (1994). Correction of partial volume inaccuracies in quantitative phase contrast MR angiography. Magnetic Resonance Imaging, 12(7), 1127-1130.

Partial Volume Effects: Calibration- CDFM

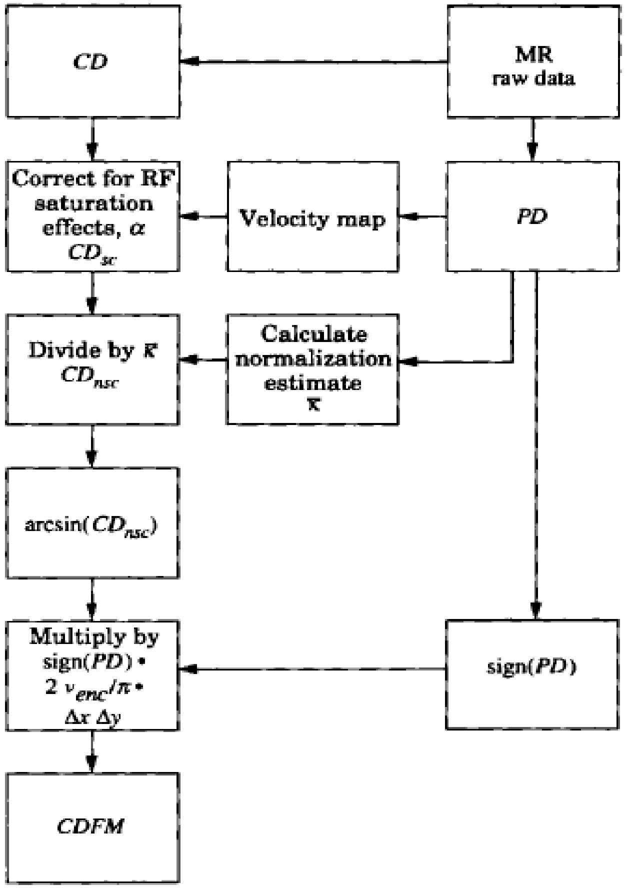

Figure 4. Flow chart for CDFM algorithm (see text for explanation of symbols).

$$\mathrm{CD} = 2\left|S_f \sin\left(\frac{\Phi_v}{2}\right)\right|$$

$$\mathrm{CD} = \kappa(x,y)\alpha\left(\theta_{flip}, v, d, TR, T1\right)\eta(x,y)\sin\left(\frac{\Phi_v}{2}\right)$$

$$CD_{sc} = \frac{CD}{\alpha[\theta_{flip}, v(PD), d, TR, T1]}$$

$$\bar{\kappa} = \frac{1}{N_{f0}}\sum_{i=1}^{N_{f0}}\frac{CD_{sc}(i)}{\sin\left[0.5PD(i)\right]}$$

$$CD_{nsc} = \frac{CD_{sc}}{\bar{\kappa}} = \eta(x,y)\sin\left(\Phi_v/2\right)$$

$$\psi = sin^{-1}(CD_{nsc}) = sin^{-1}(\eta\sin\left(\Phi_v/2\right)) = \frac{\eta\Phi_v}{2}$$

(Small angle approximation)

$$\mathrm{CDFM} = \mathrm{sign}[\mathrm{PD}(x,y)]\frac{2VENC}{\pi}\psi(x,y)\Delta x\Delta y$$

Polzin, J. A., Alley, M. T., Korosec, F. R., Gristn, T. M., Wang, Y.,... Mistretta, C. A. (1995). A complex-difference phase-contrast technique for measurement of volume flow rates. Journal of Magnetic Resonance Imaging, 5(2), 129-137.

Phase Offset Error

Sources

- Eddy current
- Concomitant Gradient
- Gradient field distortions

Results

- Small velocity offset errors often lead to much larger errors in blood flow quantification
- Such error exhibits a substantial increase with increasing distance from the isocenter of the MR system

Parameters

- Vessel position
- Imaging plane angles
- VENC

Postprocessing Correction

- Manufacturers: ROI in stationary tissue
- Estimate offset error in distant stationary tissue- spatially fitting
- Repeating the imaging sequence in “phantom”-additional time
- Magnetic field monitoring

Phase Offset Error: Correction -Spatially Fitting

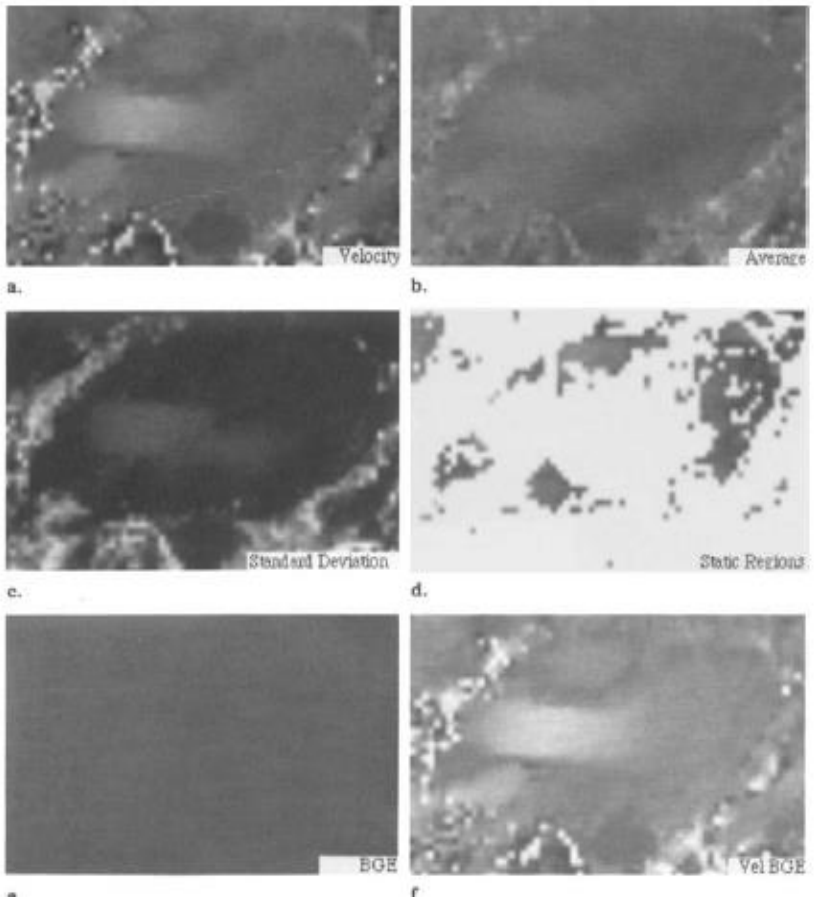

$$V_{mean}(x,y) = \frac{1}{N}\sum_{n=1}^{N} V(x,y,n)$$

$$V_{sd}(x,y) = \sqrt{\frac{1}{N}\sum_{n=1}^{N}[V_{mean}(x,y) - V(x,y,n)]^2}$$

$$V_{static}(x,y,n) = V(x,y,n) \quad if\ V_{sd}(x,y) < limit$$

$$V_{error}(x,y,n) = Ax + By + D$$

$$V_{bge}(x,y,n) = V(x,y,n) - V_{error}(x,y,n)$$

$$\mathrm{B} = \frac{[(C_{zx} \times C_{xy}) - (C_{zy} \times C_{xx})]}{[(C_{xy} \times C_{xy}) - (C_{yy} \times C_{xx})]}$$

$$\mathrm{A} = \frac{[C_{zx} - (B \times C_{xy})]}{C_{xx}}$$

$$\mathrm{D} = \mathrm{Z} - \mathrm{AX} - \mathrm{BY}$$

$$\mathrm{I} = \sum i,\ \mathrm{J} = \sum j,\ \mathrm{X} = \sum x,\ \mathrm{Y} = \sum y,\ C_{ij} = P(n) \times I \times J - (I \times J)$$

$$\mathrm{Z} = \sum V_{static}(x,y,n)$$

Walker, P. G., Cranney, G. B., Scheidegger, M. B., Waseleski, G., Pohost, G. M., & Yoganathan, A. P. (1993). Semiautomated method for noise reduction and background phase error correction in MR phase velocity data. Journal of Magnetic Resonance Imaging, 3(3), 521–530.

Phase Offset Error: Correction -Magnetic Field Monitoring

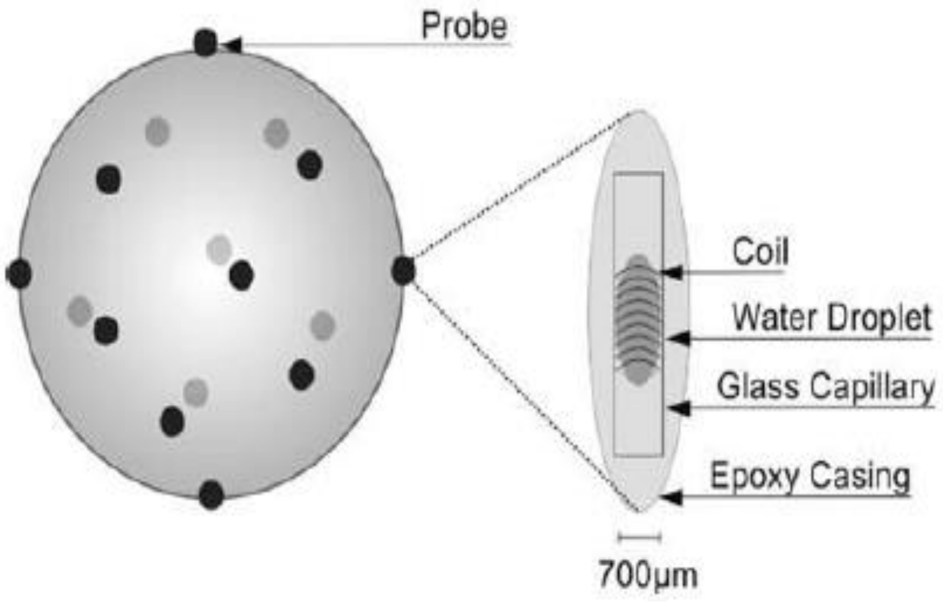

$$\vec{k}(\mathrm{t}) = \gamma \int_0^t \vec{G}(\tau)d\tau = \gamma\overrightarrow{M_0}(t)$$

$$\overrightarrow{k_v}(\mathrm{t}) = \gamma \int_0^t \vec{G}(\tau)\tau d\tau = \gamma\overrightarrow{M_1}(t)$$

$$\Delta\varphi(\vec{r}) = \angle \frac{\int s(\vec{k}, \overrightarrow{k_v} + \Delta\overrightarrow{k_v})e^{j\vec{k}\vec{r}}d\vec{k}}{\int s(\vec{k}, \overrightarrow{k_v})e^{j\vec{k}\vec{r}}d\vec{k}}$$

$$= \Delta k_v v(\vec{r}) + \Delta\varphi_e(\vec{r}, \Delta\overrightarrow{k_v})$$

$$\mathrm{v}(\vec{r}) = \frac{1}{\Delta k_v}\Delta\varphi(\vec{r})$$

$$= \frac{VENC}{\pi}\left(\Delta\varphi_v(\vec{r}) + \Delta\varphi_e\left(\vec{r}, \Delta\overrightarrow{k_v}\right)\right)$$

$$\Delta\varphi_e(\overrightarrow{r_P}) = \sum_{;=1}^{N} P_l(\overrightarrow{r_P})\,\Delta k_l$$

Giese, D. , Haeberlin, M. , Barmet, C. , Pruessmann, K. P., Schaeffter, T. and Kozerke, S. (2012), Analysis and correction of background velocity offsets in phase-contrast flow measurements using magnetic field monitoring. Magn. Reson. Med., 67: 1294-1302.

Phase Unwrapping

Path integration (Itoh,1982)

1D

$$\Delta\phi_n = \phi_n - \phi_{n-1}$$

$$\Delta\psi_n = \psi_n - \psi_{n-1}$$

Smoothness condition:

$$|\Delta\phi_n| \leq \pi$$

then:

$$\Delta\phi_n = W(\Delta\psi_n)$$

2D

$$\Delta_x\phi_{m,n} = \phi_{m,n} - \phi_{m-1,n}$$
$$\Delta_y\phi_{m,n} = \phi_{m,n} - \phi_{m,n-1}$$
$$\Delta_x\psi_{m,n} = \psi_{m,n} - \psi_{m-1,n}$$
$$\Delta_y\psi_{m,n} = \psi_{m,n} - \psi_{m,n-1}$$

Smoothness condition:

$$\left|\Delta_x\phi_{m,n}\right| \leq \pi, \qquad \left|\Delta_y\phi_{m,n}\right| \leq \pi$$

then:

$$\Delta_x\phi_{m,n} = W(\Delta_x\psi_{m,n})$$
$$\Delta_y\phi_{m,n} = W(\Delta_y\psi_{m,n})$$

Ying, L. , Liang, Z. P. , Munson, D. C. , Koetter, R. , & Frey, B. J. . (2005). Unwrapping of mr phase images using a markov random field model. IEEE Transactions on Medical Imaging, 25(1), 128-136.

Phase Unwrapping

Dual-VENC Unwrapping

$$VENC_L = \beta VENC_H, 0 < \beta < 1$$

$$\phi = A\boldsymbol{v}$$

$$\boldsymbol{v}_{Venc,H} = A^{-1}_{Venc,H}\phi_{Venc,H}$$

$$A = \frac{\pi}{\gamma V_{enc}}\begin{bmatrix} 1 & 0 & 0 \\ 0 & 1 & 0 \\ 0 & 0 & 1 \end{bmatrix}$$

$$\boldsymbol{n} = NI\left(\frac{A_{Venc,L}\boldsymbol{v}_{Venc,H} - \phi_{Venc,L}}{2\pi}\right)$$

$$\boldsymbol{v}_{Venc,L} = A^{-1}_{Venc,L}(\phi_{Venc,L} + 2\pi\boldsymbol{n})$$

Loecher, M. , & Ennis, D. B. . (2017). Velocity reconstruction with nonconvex optimization for low-velocity-encoding phase-contrast mri. Magnetic Resonance in Medicine.

Minimize TE

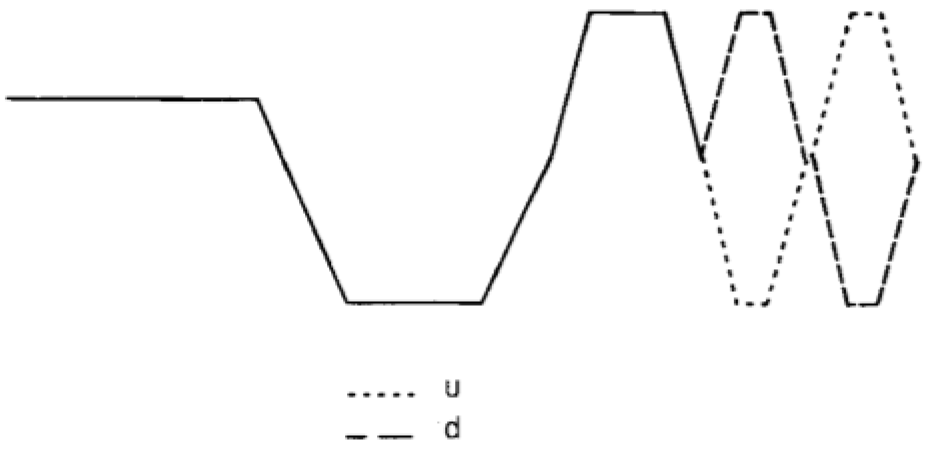

a.

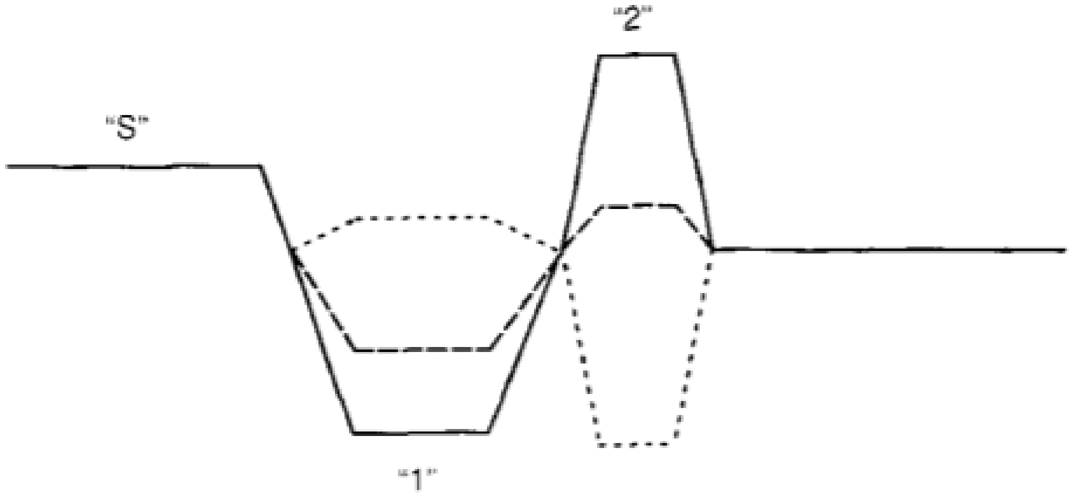

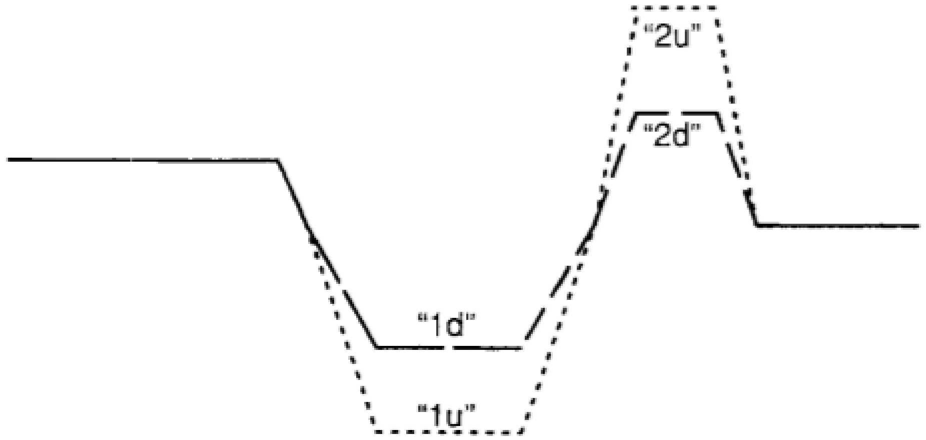

b.

$$-M_s - 0.5A_{1u}w_1 + A_{2u}(w_1 + 0.5w_2) = M_{1u}$$

$$-M_s - 0.5A_{1d}w_1 + A_{2d}(w_1 + 0.5w_2) = M_{1d}.$$

$$A_{2u} = \left[-(A_s + A_e + 2hr) + \sqrt{(A_s + A_e + 2hr)^2 + 8h\Delta M}\right]/4.$$

Bernstein, M. A. , Shimakawa, A. , & Pelc, N. J. . (1992). Minimizing te in moment-nulled or flow-encoded two-and three-dimensional gradient-echo imaging. Journal of magnetic resonance imaging : JMRI, 2(5), 583-588.

Minimize TE

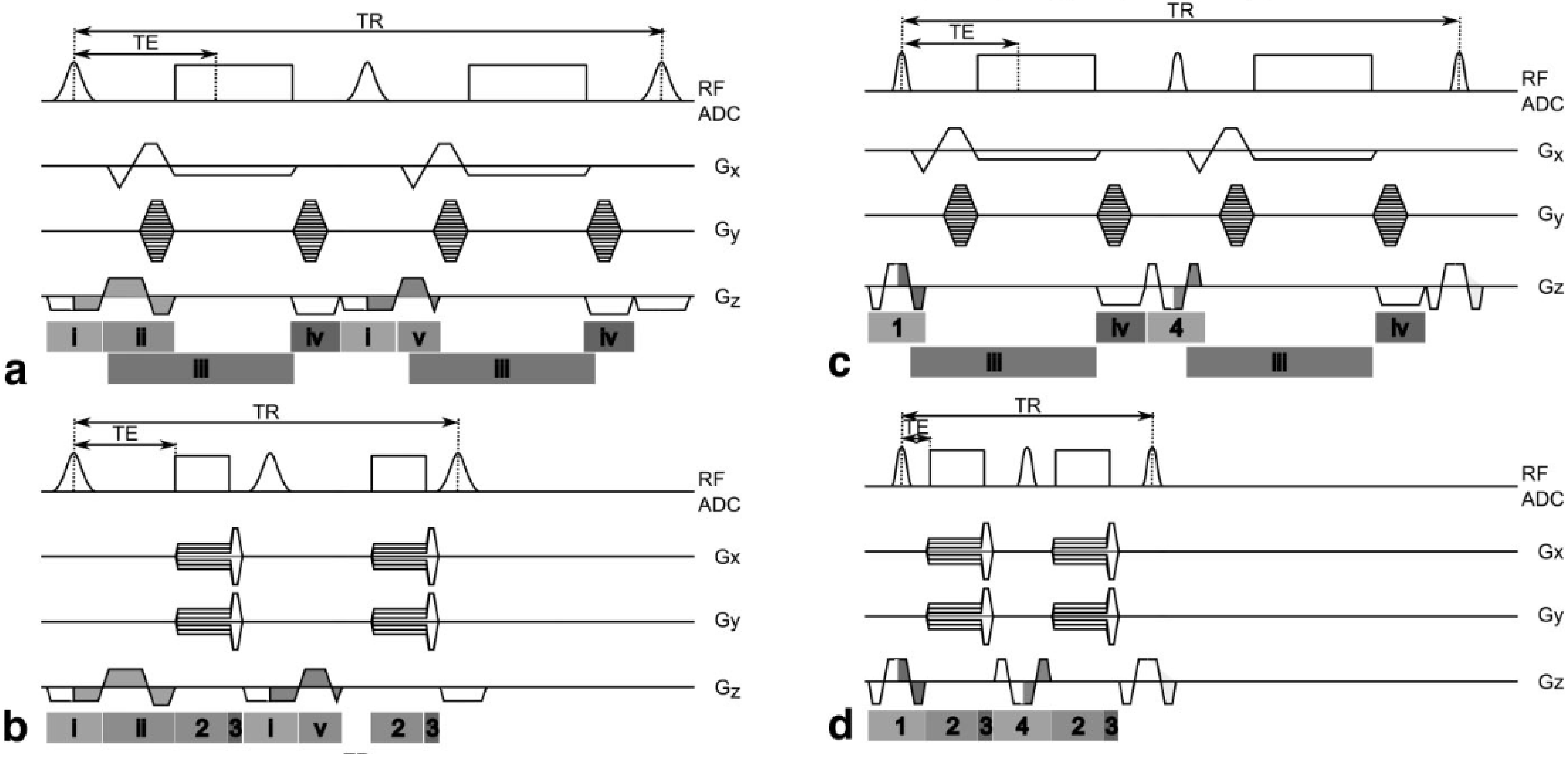

O'Brien, K. R. , Myerson, S. G. , Cowan, B. R. , Young, A. A. , & Robson, M. D. . (2009). Phase contrast ultrashort te: a more reliable technique for measurement of high-velocity turbulent stenotic jets. Magnetic Resonance in Medicine, 62(3), 626-636.

References

1. Bernstein, M. A., King, K. F., & Zhou, X. J. (2004). Handbook of MRI pulse sequences. Elsevier Academic Press.
2. Markl, M., Frydrychowicz, A., Kozerke, S., Hope, M., & Wieben, O. (2012). 4D flow MRI. Journal of Magnetic Resonance Imaging, 36(5), 1015-1036. doi:10.1002/jmri.23632
3. Funai, A. K., Fessler, J. A., Yeo, D. T. B., Olafsson, V. T., & Noll, D. C. (2008). Regularized Field Map Estimation in MRI. IEEE Transactions on Medical Imaging, 27(10), 1484-1494. doi:10.1109/TMI.2008.923956
4. Ong, F., Cheng, J., & Lustig, M. (2017). General Phase Regularized Reconstruction using Phase Cycling. arXiv e-prints. Retrieved from https://ui.adsabs.harvard.edu/abs/2017arXiv170905374O
5. Mansfield, P., & Chapman, B. (1986). Active magnetic screening of coils for static and time-dependent magnetic field generation in NMR imaging. *Journal of Physics E: Scientific Instruments, 19*(7), 540-545. doi:10.1088/0022-3735/19/7/008
6. Weavers, P. T., Tao, S., Trzasko, J. D., Frigo, L. M., Shu, Y., Frick, M. A., . . . Bernstein, M. A. (2018). B0 concomitant field compensation for MRI systems employing asymmetric transverse gradient coils. Magnetic Resonance in Medicine, 79(3), 1538-1544. doi:10.1002/mrm.26790

References

1. Tang, C. , Blatter, D. D. and Parker, D. L. (1993), Accuracy of phase-contrast flow measurements in the presence of partial-volume effects. J. Magn. Reson. Imaging, 3: 377-385.
2. Tang, C. , Blatter, D. D. and Parker, D. L. (1995), Correction of partial-volume effects in phase-contrast flow measurements. J. Magn. Reson. Imaging, 5: 175-180.
3. Hamilton, C. A. (1994). Correction of partial volume inaccuracies in quantitative phase contrast MR angiography. Magnetic Resonance Imaging, 12(7), 1127-1130.
4. Polzin, J. A., Alley, M. T., Korosec, F. R., Gristn, T. M., Wang, Y.,... Mistretta, C. A. (1995). A complex-difference phase-contrast technique for measurement of volume flow rates. Journal of Magnetic Resonance Imaging, 5(2), 129-137.
5. Walker, P. G., Cranney, G. B., Scheidegger, M. B., Waseleski, G., Pohost, G. M., & Yoganathan, A. P. (1993). Semiautomated method for noise reduction and background phase error correction in MR phase velocity data. Journal of Magnetic Resonance Imaging, 3(3), 521–530.
6. Lankhaar, J., Hofman, M. B. M., Marcus, J. T., Zwanenburg, J. J. M., Faes, T. J. C.,... Vonk-Noordegraaf, A. (2005). Correction of phase offset errors in main pulmonary artery flow quantification. Journal of Magnetic Resonance Imaging, 22(1), 73-79.
7. Chernobelsky, A., Shubayev, O., Comeau, C. R., & Wolff, S. D. (2007). Baseline Correction of Phase Contrast Images Improves Quantification of Blood Flow in the Great Vessels. Journal of Cardiovascular Magnetic Resonance, 9(4), 681–685.
8. Caprihan, A., Altobelli, S. ., & Benitez-Read, E. (1990). Flow-velocity imaging from linear regression of phase images with techniques for reducing eddy-current effects. Journal of Magnetic Resonance (1969), 90(1), 71–89.

References

9. Giese, D. , Haeberlin, M. , Barmet, C. , Pruessmann, K. P., Schaeffter, T. and Kozerke, S. (2012), Analysis and correction of background velocity offsets in phase-contrast flow measurements using magnetic field monitoring. Magn. Reson. Med., 67: 1294-1302.

10. Nayak, K. S., Nielsen, J., Bernstein, M. A., Markl, M., D. Gatehouse, P., M. Botnar, R.,… Raman, S. V. (2015). Cardiovascular magnetic resonance phase contrast imaging. Journal of Cardiovascular Magnetic Resonance, 17(1), 71.

11. Holland, B. J., Printz, B. F., & Lai, W. W. (2010). Baseline correction of phase-contrast images in congenital cardiovascular magnetic resonance. Journal of Cardiovascular Magnetic Resonance, 12(1), 11.

12. Gatehouse, P. D., Rolf, M. P., Bloch, K. M., Graves, M. J., Kilner, P. J., Firmin, D. N.,… Hofman, M. B. (2012). A multi-center inter-manufacturer study of the temporal stability of phase-contrast velocity mapping background offset errors. Journal of Cardiovascular Magnetic Resonance, 14(1), 72.

References

1. Itoh, K. . (1982). Analysis of the phase unwrapping algorithm. *Applied Optics, 21*(14), 2470.
2. Ying, L. , Liang, Z. P. , Munson, D. C. , Koetter, R. , & Frey, B. J. . (2005). Unwrapping of mr phase images using a markov random field model. *IEEE Transactions on Medical Imaging,25*(1), 128-136.
3. Arevalillo-Herráez M, Gdeisat, M. A. , & Burton, D. R. . (2009). Hybrid robust and fast algorithm for three-dimensional phase unwrapping. *Applied Optics, 48*(32), 6313-23.
4. Loecher, M. , & Ennis, D. B. . (2017). Velocity reconstruction with nonconvex optimization for low-velocity-encoding phase-contrast mri. Magnetic Resonance in Medicine..
5. Carrillo, H., Osses, A., Uribe, S., & Bertoglio, C. (2019). Optimal Dual-VENC Unwrapping in Phase-Contrast MRI. *IEEE Transactions on Medical Imaging, 38*(5), 1263-1270.
6. Bernstein, M. A. , Shimakawa, A. , & Pelc, N. J. . (1992). Minimizing te in moment-nulled or flow-encoded two-and three-dimensional gradient-echo imaging. Journal of magnetic resonance imaging : JMRI, 2(5), 583-588.
7. O'Brien, K. R. , Myerson, S. G. , Cowan, B. R. , Young, A. A. , & Robson, M. D. . (2009). Phase contrast ultrashort te: a more reliable technique for measurement of high-velocity turbulent stenotic jets. Magnetic Resonance in Medicine, 62(3), 626-636.